



HAL
open science

Gas emissions due to magma-sediment interactions during flood magmatism at the Siberian Traps: gas dispersion and environmental consequences.

Giada Iacono-Marziano, Virginie Marecal, Michel Pirre, Fabrice Gaillard, Joaquim Arteta, Bruno Scaillet, Nicholas Arndt

► To cite this version:

Giada Iacono-Marziano, Virginie Marecal, Michel Pirre, Fabrice Gaillard, Joaquim Arteta, et al.. Gas emissions due to magma-sediment interactions during flood magmatism at the Siberian Traps: gas dispersion and environmental consequences.. Earth and Planetary Science Letters, 2012, 357-358, pp.308-318. 10.1016/j.epsl.2012.09.051 . insu-00801929

HAL Id: insu-00801929

<https://insu.hal.science/insu-00801929v1>

Submitted on 18 Mar 2013

HAL is a multi-disciplinary open access archive for the deposit and dissemination of scientific research documents, whether they are published or not. The documents may come from teaching and research institutions in France or abroad, or from public or private research centers.

L'archive ouverte pluridisciplinaire **HAL**, est destinée au dépôt et à la diffusion de documents scientifiques de niveau recherche, publiés ou non, émanant des établissements d'enseignement et de recherche français ou étrangers, des laboratoires publics ou privés.

**Gas emissions due to magma-sediment interactions during flood magmatism at the
Siberian Traps: gas dispersion and environmental consequences.**

Giada IACONO-MARZIANO^{1*}, Virginie MARECAL², Michel PIRRE³, Fabrice
GAILLARD¹, ARTETA Joaquim², Bruno SCAILLET¹, and Nicholas T. ARNDT⁴

¹ ISTO, UMR 7327 CNRS-Université d'Orléans, Orléans, France

² CNRM-GAME, URA1357, Météo-France and CNRS, Toulouse, France

³ LPC2E, UMR 6115 CNRS-Université d'Orléans, Orléans, France

⁴ ISTerre, Université de Grenoble, Grenoble, France

* Corresponding author: Giada.Iacono@cnsr-orleans.fr, 1A rue de la Férollerie 45071 Orléans
cedex 2, France. Tel: 0033238257868. Fax: 0033238636488.

Abstract

We estimate the fluxes of extremely reduced gas emissions produced during the emplacement of the Siberian Traps large igneous province, due to magma intrusion in the coaliferous sediments of the Tunguska Basin. Using the results of a companion paper (Iacono-Marziano et al. submitted to EPSL), and a recent work about low temperature interaction between magma and organic matter (Svensen et al., 2009), we calculate CO-CH₄-dominated gas emission rates of 7×10^{15} - 2×10^{16} g/yr for a single magmatic/volcanic event. These fluxes are 7 to 20 times higher than those calculated for purely magmatic gas emissions, in the absence of interaction with organic matter-rich sediments. We investigate, by means of atmospheric modelling employing present geography of Siberia, the short and mid term dispersion of these gas emissions into the atmosphere. The lateral propagation of CO and CH₄ leads to an

important perturbation of the atmosphere chemistry, consisting in a strong reduction of the radical OH concentration. As a consequence, both CO and CH₄ lifetimes in the lower atmosphere are enhanced by a factor of at least 3, at the continental scale, as a consequence of 30 days of magmatic activity. The short-term effect of the injection of carbon monoxide and methane into the atmosphere is therefore to increase the residence times of these two species and, in turn, their capacity of geographic expansion. The estimated CO and CH₄ volume mixing ratios (i.e. the number of molecules of CO or CH₄ per cm³, divided by the total number of molecules per cm³) in the low atmosphere are 2-5 ppmv at the continental scale and locally higher than 50 ppmv. The dimension of the area affected by these high volume mixing ratios decreases in the presence of a lava flow accompanying magma intrusion at depth. Complementary calculations for a 10-year duration of the magmatic activity suggest (i) an increase in the mean CH₄ volume mixing ratio of the whole atmosphere up to values 3 to 15 times higher than the current one, and (ii) recovery times of 100 years to bring back the atmospheric volume mixing ratio of CH₄ to the pre-magmatic value. Thermogenic methane emissions from the Siberian Traps has already been proposed to crucially contribute to end Permian-Early Triassic global warming and to the negative carbon isotopic shift observed globally in both marine and terrestrial sediments. Our results corroborate these hypotheses and suggest that concurrent high temperature CO emissions also played a key role by contributing to increase (i) the radiative forcing of methane and therefore in its global warming potential, and (ii) the input of isotopically light carbon into the atmosphere that generated the isotopic excursion. We also speculate a poisoning effect of high carbon monoxide concentrations on end-Permian fauna, at a local scale.

Keywords: Siberian Traps, magma-organic matter interaction, gas emissions, carbon monoxide, methane, atmospheric modelling.

1. Introduction

Large Igneous Provinces (LIPs) are enormous crustal emplacements (millions of km³) of predominantly mafic extrusive and intrusive rocks originating via processes other than “normal” seafloor spreading, e.g. continental flood basalts (or traps), volcanic passive margins, oceanic plateaus, and seamount groups (Coffin and Eldholm, 1994). In 1972 Vogt noted that the end-Cretaceous mass extinction was synchronous with the eruption of the Deccan Traps. Since then the idea that LIP eruption times coincide with major mass extinctions has been broadened and several other cases have been documented (Courtilot and Renne, 2003). The extinctions have been ascribed to both short and long term effects of magmatic gas emissions (e.g. Vogt, 1972; Axelrod, 1981; Cockell, 1999; Retallack, 1999). As noted by Wignall (2001) and Ganino and Arndt (2009) among others, the main problem with such a hypothesis is that the volume of erupted magma is not correlated with the magnitude of the extinction, as measured by the number of taxa that became extinct. In addition, the erupted magmas are dominantly tholeiitic basalts, a category of magma believed to be volatile-poor (Saal et al., 2001). Sobolev et al. (2011) advocate an important contribution of CO₂-HCl-dominated volatiles deriving from recycled oceanic crust in the magma source. A possible role of silicic magmas has also been invoked for sulphur emissions from LIPs, also in this case the volume of explosive products being not directly related to the importance of the environmental crisis (Scaillet and Macdonald, 2006).

To explain the lack of correlation with the volume of the magmatic products, the importance of extinctions has been linked to both the nature and amount of thermogenic gases produced during the LIP emplacement, which are controlled by the type of rocks encountered by basaltic magmas during their ascent (Svensen et al., 2004, 2007, 2009; Erwin, 2006; Retallack and Jahren, 2008; Ganino and Arndt, 2009). A growing body of evidence indicates that interactions between country rocks and magmatic sills and dikes can be particularly

important due to the long exposure to high temperatures: heating of carbonates, sulphates, salts, or organic-compounds (such as bituminous shales or coals) can inject into the atmosphere a quantity of volatiles that greatly exceeds the amount delivered by purely magmatic degassing (Svensen et al., 2004, 2007, 2009; Ganino et al., 2008; Iacono-Marziano et al., 2007, 2009). This may help explain why some traps coincide with major extinction events, while others leave almost no trace in the fossil record (Ganino and Arndt, 2009).

1.1. Siberian Traps

The Siberian Traps are the most voluminous subaerial large igneous province (LIP), which covers more than 60% of the Siberian Platform (1.5 million km²) (Reichow et al., 2002); the distribution of lavas suggests that they do not constitute a single continuous province but rather the amalgamation of several sub-provinces (Mitchell et al., 1994). The emplacement of the Siberian Traps has occurred contemporaneously to the end-Permian crisis, the most severe extinction affecting marine and continental biota (Wignall, 2001; Erwin et al., 2002), and to a strong perturbation of the Earth's carbon cycle, globally marked by a negative carbon isotope excursion recorded in marine and terrestrial carbonates and organic matter (Korte et al., 2010 and references therein). The relative timing of these events is not fully resolved, the beginning of the volcanic activity preceding the strongest isotopic excursion and the main extinction event, both, however, occurring before the main emplacement phase of the Siberian Traps (Korte et al., 2010). Siberian basaltic flows are underlain almost everywhere by terrigenous, coal-bearing sedimentary rocks of the Tunguska Basin (Fig. 1), which are absent only in a few, local-scale, tectonic structures (Czamanske et al., 1998). The 300-m-thick Late Carboniferous-Permian Tunguska coal basin is one of the largest in the world and contains numerous thick coal seams (Czamanske et al., 1998). The underlying Neoproterozoic to Carboniferous sedimentary sequence, through which basaltic magmas ascended, comprises

carbonates, shales, sandstones and, concentrated in central and southern Tunguska, evaporites. Numerous petroleum levels with regional distribution and variable thicknesses (from a few meters to 80 m) are present in the Silurian, Ordovician, Cambrian, and Neoproterozoic strata (Svensen et al., 2009; Kuznetsov, 1997). The average organic matter content of the sedimentary rocks is 1-3 wt% and can locally reach 8-22 wt% (Kuznetsov, 1997).

Important interactions between magmas and carbonaceous sediments have already been proposed by several authors to have been the major cause of the environmental impact of the Siberian Trap emplacement (Visscher et al., 2004; Retallack and Krull, 2006; Payne and Kump, 2007; Retallack and Jahren, 2008 ; Svensen et al., 2009; Retallack, 2012). Recent analyses of terrestrial carbon in marine sediments from the Canadian High Arctic have brought further evidence for high temperature magma-coal interactions at the Siberian Traps (Grasby et al., 2011). This terrestrial carbon is in the form of char and is very similar to modern fly ash produced from coal-fired power plants (combustion temperatures between 1300 and 1600°C), it has been found more than 20,000 km far from Siberia, suggesting a global dispersion of the ashes derived from the combustion of coaliferous sediments (Grasby et al., 2011). In a companion paper (Iacono-Marziano et al., submitted to EPSL) we show how the occurrence of graphite and native iron in several large intrusions belonging to the Siberian Traps indicates intense high temperature interactions between magma and coaliferous sediments, and implies extremely reduced gas emissions. The fate of these gases upon reaching the atmosphere is a crucial point to elucidate, in order to estimate their potential environmental impact.

In this paper we estimate the fluxes of unusually reduced gases that could have been produced during a single magmatic event of the Siberian Traps. To investigate the short and long term dispersion of these gases into the atmosphere we use atmospheric modelling coupling gas transport and chemistry, a methodology applied for the first time to volcanic gas emissions.

2. Methods

2.1 Quantification of gas emissions due to magma-sediment interactions

We use the gas compositions estimated by Iacono-Marziano et al. (submitted to EPSL) to characterize the degassing that may have occurred at the Siberian Traps during the emplacement of native iron-bearing intrusions. The quantification of these emissions requires the knowledge of the amount of magma involved in organic matter assimilation. Field evidence in the Northern Tunguska Basin (Ryabov and Lapkovsky, 2010) suggests that magma-coal interaction persisted for an entire intrusive event, which led to multiple 40-110 m thick intrusions containing native iron. Native iron ores have been generally observed in the shallower part of the intrusions, in agreement with our calculations predicting native iron saturation at pressures lower than 10 MPa.

Current estimations of magma production rates for the Siberian Traps, as for all other traps, are very imprecise, owing to the uncertainties related to event size, and the small number of precise ages available for most events (Ernst et al., 2005). Chenet et al. (2008) estimated a magma eruption rate for single effusive events of the Deccan Traps of $\sim 100 \text{ km}^3/\text{yr}$. The only large basaltic eruption occurred in historical times that could be regarded as a proxy for LIPs' events is the 1783-4 Laki eruption: it lasted ~ 8 months and produced 15 km^3 of basalts (Thordarson and Self, 2003). The mean magma eruption rate was equivalent to $22 \text{ km}^3/\text{yr}$, with peak magma discharges equivalent to $157\text{-}208 \text{ km}^3/\text{yr}$ (Thordarson and Self, 2003). Although the relation between magma intrusion and extrusion rates is still barely constrained, we can reasonably use a magma production rate of $100 \text{ km}^3/\text{yr}$ to estimate gas emissions resulting from high temperature coal assimilation during the emplacement of Siberian intrusions.

Two scenarios are simulated: magma intrusion without lava production at surface, and magma intrusion associated with lava flows. The occurrence of effusive activity concurrent to the formation of native iron-bearing intrusions has not been clearly demonstrated, effusive products being generally absent in these areas (Ryabov and Lapkovsky, 2010). However, the discovery of substantial amounts of coal combustion derived char 20,000 km away from the Siberian Traps (Grasby et al., 2011) indicates that, at least in a certain period of the Siberian Trap emplacement, magma-coal interactions have been associated to magma extrusion at surface.

When the emplacement of a lava flow accompanies magma intrusion at depth, an additional process is most likely significant in the Siberian Trap context, i.e. atmospheric nitrogen fixation at the lava surface. Hot lava flows have been observed to fix atmospheric nitrogen at their surface following (Huebert et al., 1999):



The production of NO is proportional to the temperature at which the nitrogen oxidation occurs (Mather et al., 2004). At 1200 and 1400 K (a good approximation of the surface temperature of an advancing lava flow; Huebert et al., 1999), the molar fraction of NO generated by this mechanism in volcanic gases has been calculated to be 2×10^{-4} and 6×10^{-4} , respectively (Mather et al., 2004).

A further complication in the case of Siberian intrusions is represented by the presence of a thick sequence of sedimentary carbonates and possibly evaporites beneath the coal measures (Svensen et al., 2009; Czamanske et al., 1995, 1998). Interaction of the basaltic magma with carbonate rocks may have produced large quantities of CO₂ by high-temperature assimilation or breakdown of carbonates (Svensen et al., 2009; Iacono-Marziano et al., 2007, 2009). Heating of evaporitic rock most likely generates SO₂ and halocarbons (Svensen et al., 2009), however the stratigraphy of the northern part of the Tunguska Basin (where native iron

bearing intrusions occur) generally do not include evaporites (Fig. 1) (Matukhin, 1991; Petrychenko et al., 2005). It is difficult to discriminate the fraction of these gases that is driven off from the metamorphic aureoles ascending in pipe-like structures (Svensen et al., 2009), from that coexisting with the magma. Gases vented by the pipes are directly released in the atmosphere, our approach not allowing any estimates of the gas quantity released. On the contrary, gases that ascend in equilibrium with the magma are reduced upon interaction with coal forming the CO-dominated gas mixtures described above (sulphur remaining soluble in the magma). In this case, interactions with sedimentary carbonates and evaporites prior to reaction with coal would increase the amount of oxygen available in the magma (O^{magma} in reaction 1 and 2 in Iacono-Marziano et al., submitted to EPSL) and therefore increase its potential to assimilate organic matter and increase in the amount of CO produced, the presence of CO_2 and SO_2 being precluded in a gas phases in equilibrium with native Fe.

2.2 Atmospheric modelling

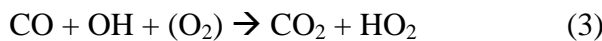
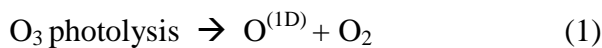
Atmospheric modelling was used to evaluate (i) whether the extremely reduced gases, produced during intrusive (possibly accompanied by extrusive) activity, persist in the lower atmosphere without being oxidised or conveyed to the stratosphere, (ii) which concentration and lifetime they can attain close to the Earth's surface. Our approach is similar to the one employed for 1783 Laki eruption (Chenet et al., 2005): we use a regional 3D atmospheric model, which includes the transport of trace gases (Freitas et al., 2009), to simulate the atmospheric dispersion of the emitted gases at a continental scale, after 30 days of magmatic activity. Differently from Chenet et al. (2005), who investigate the dispersion of sulphates and tephra, our model is coupled to a tropospheric chemistry model to study the chemical modifications of the emitted reactive volcanic gases as they mix with the surrounding

atmosphere. The chemical scheme includes photochemical reactions to describe the chemistry of CH₄, CO, H₂, O₃, NO_x (NO+NO₂) and HO_x (OH+HO₂).

The CATT-BRAMS model (Freitas et al., 2009) used for atmospheric simulations is a state-of-the-art regional 3D model including all major atmospheric processes such as radiation (radiative code of the Community Aerosol and Radiation Model for Atmospheres, Toon et al., 1989), turbulence (Mellor and Yamada, 1982), surface-atmosphere interaction (Walko and Tremback, 2005), convection (Grell, 1993; Grell and Dévényi, 2002) and microphysical processes (Walko et al., 1995) leading to cloud and precipitation formation.

For the present study an atmospheric chemistry module is coupled to the CATT-BRAMS model. This chemistry module includes a comprehensive set of 12 photolysis reactions and 43 gaseous chemistry reactions of 19 species (CO, CH₄, H₂, O₃, O^(3P), O^(1D), NO, NO₂, NO₃, HNO₃, HNO₄, N₂O₅, HONO, OH, HO₂, H₂O₂, HCHO, CH₃O₂ and CH₃OOH), describing the photochemistry of CO, CH₄, O₃, NO_x (NO+NO₂) and HO_x (OH+HO₂).

In this study we focus on CO and CH₄ concentrations, expressed as volume mixing ratios (i.e. the number of molecules of CO or CH₄ per cm³, divided by the total number of molecules per cm³), and lifetimes. CO and CH₄ concentrations and lifetimes both depend on the OH concentration, mainly resulting from the following reactions:



where O^(1D) is the excited state of the oxygen atom.

2.2.1 Application to the Siberian Traps

The simulations were run on a domain covering current Siberia (the studied area is limited by Urals to the West and by Tienschan, Altay, Sayan Mountains and Stanovoy range to the South and South-East) and used present geography and topography. The climate prior to the Permian–Triassic boundary was significantly warmer than today, and there is no evidence for polar climates (Chumakov and Zharkov, 2003; Roescher et al., 2011). Atmospheric temperature plays both a direct and indirect role in equations (1) to (4), and in particular affect CH₄ lifetime. However, given the uncertainty in existing estimates of pre-crisis atmospheric temperatures in the concerned area (e.g. Rees et al., 2002; Roescher et al., 2011), we preferred to use current temperature distribution in our modelling, and to run our simulations during the whole month of July. July is the time of the year when photolysis chemistry is most active because of intense solar radiation. Therefore it is in summer that OH production is most important leading to expected significant modifications of CO and CH₄ lifetimes.

Several global climatic models employed end-Permian paleogeography to estimate the effect of increased concentrations of greenhouse gases in the atmosphere (e.g. Kiehl and Shields, 2005; Roscher et al., 2011). Differently from these models that considers inert greenhouse gases, we deal with the chemical reactions of the main reactive species of the atmosphere. In this sense, the originality of our modelling is that it can estimate the impact at the regional scale of “modified” magmatic gas emissions on the reactivity of the atmosphere and therefore on the lifetime of its constituents, like methane and carbon monoxide.

The polar stereographic projection used leads to a horizontal grid spacing of ~14 km by ~14 km. The model domain extends vertically from surface up to 21 km with a vertical grid-spacing increasing with altitude: the thickness of the lowest layer (close to the surface) is 30 m, while that of the upper layer (in the lower stratosphere) is 1 km.

For the meteorological variables, the model initialisation and the boundary conditions are prescribed from the European Centre for Medium-range Weather Forecasts (ECMWF)

operational analysis for 2008. This year was chosen randomly since the climatologic conditions prevailing at the end of the Permian are not precisely known, but they may have been similar to the actual ones (Rees et al., 2002). Note that the choice of a different year would not change the main conclusions of this study.

To initialize the photochemistry module, the volume mixing ratio of CH₄ is assumed to be 500 ppbv, the mean value that was prevailing before the industrial period (Fischer et al., 2008). In the troposphere, the CO volume mixing ratio is set initially to 50 ppbv, the NO_y (HNO₃ + NO + NO₂ + NO₃ + HNO₄ + N₂O₅ + HONO) volume mixing ratio is set to 0.5 ppbv and the ozone volume mixing ratio to 10 ppbv corresponding to present-day not polluted area. Water vapour is a prognostic variable computed by the atmospheric model.

The parameters that are injected in the model are the emitted volatile species, and the geometry and geographical location of the emission zone. The magmatic/volcanic volatile species considered are: CH₄, CO, H₂, H₂O, NO with the annual fluxes estimated in Table 1. We do not include CO₂ emissions in our atmospheric simulations because (i) we have no constraints to precisely quantify CO₂ produced by magma-carbonate interactions (see section 3.1), and (ii) they do not influence the lifetimes of CO and CH₄ and therefore their dispersion into the atmosphere. CO₂ lifetime in the atmosphere is extremely long, therefore an increase in CO₂ concentration would not change our results for CO and CH₄. The photochemical loss reaction of CO₂:



is only significant in the upper atmosphere, and negligible in the lower atmosphere.

The emission zone was considered ~210 km long and ~14 km wide, in agreement with the total area of native iron-bearing intrusions currently outcropping (Ryabov and Lapkovsky, 2010); this choice has a negligible influence on gas dispersion in the absence of a lava flow, but an important role (discussed below) in the presence of it. The emission zone has been

centred at 64°N, 96°E, in agreement with the current location of the Siberian Traps, as the latitude of the Siberian platform at the end of the Permian was likely similar to the actual one (Rees et al., 2002). Apart from volcanic emissions, present natural emissions of CO and NO are also taken into account. They come from monthly mean data from the GEIA (Global Emissions Inventory Activity) database (<http://www.geiacenter.org/>) and represent present-day natural emissions since we do not have information on natural emissions at the end of the Permian.

Two scenarios are simulated: magma intrusion without lava production at surface, and magma intrusion associated with lava flows. In the case of magma intrusion without lava production at surface, we assume that there is no heat flux from the surface to the atmosphere. Two simulations of 30 days were run for minimum and maximum gas fluxes (first and second column in Table 1, respectively). The occurrence of a lava flow heats the atmosphere, inducing a temperature perturbation expected to favour convective vertical transport of gas emissions and thus to have significant effects on gas dispersion. Moreover convection leads to the formation of clouds, which affect photolysis rates due to their filtering effect on solar radiation. We run an additional simulation of 30 days for minimum gas fluxes (third column in Table 1). We used a heat flux of $5.5 \cdot 10^3 \text{ W m}^{-2}$ proposed by Kaminski et al. (2010), from which we derived a temperature perturbation applied to the first atmospheric model layer above surface at each model time step. The intensity of the temperature perturbation strictly depends on the geometry of the emission zone, i.e. the area of the lava flow: the larger the emission zone, the more significant the temperature perturbation. Due to the lack of information about the size of a possible lava flow associated to the emplacement of native iron-bearing intrusions, we only explored the case of a lava flow having the extension of the intrusions (i.e. 210 km × 14 km).

2.3 Mid-term estimations of methane concentration in the atmosphere

Complementary calculations were performed for methane to estimate the effect of 10 years lasting magmatic activity on the mean CH₄ volume mixing ratio of the whole atmosphere. Magma production rate (100 km³/yr) and consequent gas emissions (Table 1) were assumed constant during a time T and the lifetime of CH₄ constant in the atmosphere. Calculations were performed for CH₄ lifetimes of 8, 10, 15, 20 years. The initial CH₄ volume mixing ratio is assumed to be 500 ppbv, the mean value that was prevailing before the industrial period (Fischer et al., 2008). The total mass of CH₄, M(t), present in the atmosphere at time t was therefore calculated as:

$$M(t) = m_0 \tau (1 - \exp(-\frac{t}{\tau})) \quad \text{at time } t < T \quad (6)$$

$$M(t) = m_0 \tau \exp(-\frac{t}{\tau}) (\exp(\frac{T}{\tau}) - 1) \quad \text{at time } t > T \quad (7)$$

where τ is the lifetime of CH₄, and m_0 is the mass of CH₄ emitted by magmatic activity per second. Assuming that emitted CH₄ molecules fill the whole atmosphere with a uniform volume mixing ratio, the following expression can be derived:

$$\mu(t) = \frac{M(t) m_{air} g}{P_0 m_{CH_4} 4\pi R^2} \quad (8)$$

where $\mu(t)$ is CH₄ volume mixing ratio, m_{air} and m_{CH_4} are the mean molar mass of air and CH₄, respectively, g is the gravitational acceleration, P_0 is the ground pressure, and R is the earth radius. The evolution of $\mu(t)$ was investigated over 100 years, including 10 years of magmatic activity.

3. Results

3.1 Gas production potential of a single intrusive event at the Siberian Traps

As Figure 2 schematically illustrates, basaltic magmas of the Siberian Traps ascended through a thick Neoproterozoic-Permian sedimentary pile comprising carbonates, shales, sandstones, evaporites (concentrated in central and southern Tunguska), and coaliferous sediments (Svensen et al., 2009; Czamanske et al., 1998).

The composition of the gas phase is dictated by the presence of native iron that constrains the fO_2 of the magma and coexisting gases to be $< FMQ-6$: these conditions preclude the presence of “classical” volcanic gases dominated by H_2O , CO_2 and SO_2 (Iacono-Marziano et al., submitted to EPSL). In particular, sulphur emissions are extremely low in proportion (SO_2 , but also H_2S and S_2). For the emplacement of Siberian native iron-bearing intrusions, we estimate that the amount of CO produced varied between 3 and 12 Gt/yr (Table 1). These fluxes are exceptional when compared to current CO emissions of anthropogenic origin that have been estimated to be ~ 1 Gt for the year 2000 (EDGAR database, <http://edgar.jrc.ec.europa.eu>). The corresponding annual consumption of coal is $\sim 1-2$ km³, which is a negligible amount in front of the coal resources of the Tunguska basin ($>10^6$ km², ~ 1850 Gt; Akulov, 2006).

When magma intrusion is not associated with lava flows, high temperature gases could be affected by cooling after separation from the magma, therefore modifying their composition CO to $H_2O-CH_4-CO_2$ dominated (Iacono-Marziano et al., submitted to EPSL). Assessing the amount of cooling is extremely difficult, as several parameters are not precisely known, such as the actual depth of formation of native iron bearing intrusions, the volumes of involved magma, and the thermal conditions of host rocks. On the contrary, gas cooling is unlikely to occur when gas ascent is accompanied by magma rising to form a lava flows at surface. We will not take into account the effect of gas cooling either in the case of magma intrusion without or with associated lava flow.

In the case of magma intrusion accompanied by lava flows, gas emissions are slightly richer in carbon monoxide and depleted in the other species (Table 1). This is due to the difference in the degassing pressure, which is 10 MPa in the case of shallow intrusions (Iacono-Marziano et al., submitted to EPSL), and 0.1 MPa when the magma reaches the surface to feed a lava flow. The amount of NO calculated to be produced by atmospheric nitrogen fixation at the lava surface varies between 1 and 5×10^{12} g/yr NO, depending on the surface temperature of the lava flow (Mather et al., 2004).

A likely additional contribution to CO-dominated gas emissions is represented by CO₂-dominated gases produced by the assimilation of carbonate rocks occurring at higher depths than that of coal sediments (Fig.2). SO₂ and halocarbon emissions by assimilation of evaporitic rocks are less probable in the area of native iron-bearing intrusions (see section 2.1 and Fig.2). When CO₂ produced by carbonate assimilation coexists with the ascending magma, it increases magma potential to assimilate organic matter and produce CO. For instance, an initial CO₂ content of 2 wt% (instead of 0.24 wt%) prior to organic matter incorporation, implies that ~1.2 wt% organic matter (instead of ~0.5 wt%) is necessary to reach saturation in both graphite and native iron at 10 MPa, yielding 3.4 wt% CO in the magma (instead of 1.0 wt%). We cannot precisely estimate this additional contribution to CO emissions, given the extreme difficulty to quantify the amount of CO₂ produced by magma-carbonate interactions and the portion of this CO₂ that coexist with the magma upon its ascent. More generally, interactions with carbonates and evaporites and their gas production potential will be neglected here, due to the lack of constraints to precisely quantify them.

On the contrary, the contribution of contact metamorphism of organic matter-rich sedimentary rocks to gas emissions has been estimated for the Siberian Traps (Svensen et al., 2009). Low-temperature destabilization of hydrocarbons in the contact aureoles leads to methane emissions between 12,300 and 37,000 Gt at the basin scale (Svensen et al., 2009). From these

emissions (*tot CH₄*), considering a magma production rate (*MPR*) of 100 km³/yr (Chenet et al., 2008), and a total magma volume (*TMV*) of 4×10⁵ km³ (Svensen et al. 2009), we calculate an annual CH₄ production rate during a single intrusive/eruptive event (e.g. the emplacement of native iron-bearing intrusions) as:

$$\text{CH}_4 \text{ (g/yr)} = \text{tot CH}_4 \text{ (g)} * \text{MPR (km}^3\text{/yr)} / \text{TMV (km}^3\text{)} \quad (9)$$

which is 3.1-9.3×10¹⁵ g/yr, therefore comparable to CO emissions on a yearly basis (Table 1).

Calculated gas emissions for the degassing of purely magmatic volatiles from a basaltic melt saturated in H₂O, CO₂ and S at 100 MPa is also shown in Table 1, to compare with emissions due to organic matter assimilation. Volatile contents calculated by this approach are within the range of those typically measured in basaltic melts (Jambon, 1994 and references therein; Wallace, 2005 and references therein). Table 1 clearly illustrates how coal assimilation substantially increases gas emissions and strongly modifies their composition. The total volatile yield of a single magmatic event is increased by a factor of 7 to 20, due to magma-sediment interactions and produced total fluxes reach 7×10¹⁵- 2×10¹⁶ g/yr (Table 1). Carbon monoxide becomes the dominant degassed species, overwhelming CO₂ and H₂O, while H₂ and CH₄ abundances strongly increase. We recall that a possible contribution from carbonate (and less probably evaporite) assimilation is neglected here.

3.2 CO and CH₄ dispersion

Figures 3 (a, b, c) shows the volume mixing ratio of CO in the lower layers of the atmosphere (0-30 m), 30 days after the gases produced by magma intrusion arrive at surface (the results for 10 and 20 days are shown in Fig. 1 of the Supplementary Material). Three different simulations are presented: the first two have been run using maximum (Fig.3 a) and minimum (Fig. 3 b) gas emissions calculated for magma intrusion at ~ 350-500 m depth, while the third one (Fig.3 c) employed minimum gas fluxes estimated for magmatic intrusions associated to

lava flows (third column in Table 1). In this last case, a temperature perturbation accounts for the heating effect of the lava flow (see section 2.2.1). In all cases both the magma production rate ($100 \text{ km}^3/\text{yr}$) and the consequent gas emissions (in Table 1) have been assumed constant during time.

In the three simulations, the lateral propagation of CO is significant at the continent scale within 20 days (Fig.SM1 b, e, h). After 30 days, CO volume mixing ratios ranging between 2 and 5 ppmv (typical values measured in urban areas; WHO, 2004) are observed over a zone of $\sim 30^\circ$ in longitude and 12° in latitude ($\sim 2 \times 10^6 \text{ km}^2$) for minimum gas fluxes (Fig.s 3b and 3c) and over most of the continent, for maximum gas fluxes (Fig.3a). Close to the gas production zone CO volume mixing ratios higher than 50 ppmv are locally reached. This value represents the current Permissible Exposure Limit (PEL) for 8 hours established by the World Health Organization (WHO, 2004). In the case of lava flows, the associated temperature perturbation significantly reduces the area affected by CO volume mixing ratios higher than 50 ppmv, whilst only slightly influencing the extension of the zone showing 2-5 ppmv volume mixing ratios. The impact of the lava flow on CO dispersion would increase with the area of the emission zone. Owing to the lack of evidence for lava flow accompanying magma intrusion at depth, hence on their potential extension, we did not investigate further the thermal effect on gas dispersion.

Figure 3 (d, e, f) shows CH_4 volume mixing ratio in the lower layers of the atmosphere (0-30 m) accompanying CO volume mixing ratios in Figure 3 (a, b, c). CH_4 dispersion is greater than that of CO: after 30 days that gas emissions reached the surface, the area concerned by volume mixing ratios between 2 and 5 ppmv covers most of the continent, for the three simulations (Fig.s 3 d, e, f). Similarly to CO, the effect of the lava flow is to reduce CH_4 volume mixing ratios close to the emission zone (Fig.3f).

3.3 CO and CH₄ lifetimes

The horizontal propagation of CO and CH₄ far from the degassing area leads to a significant perturbation of the atmosphere chemistry at the continental scale, consisting in a strong reduction of the radical OH concentration and therefore a decrease in the oxidizing potential of the atmosphere. Both CO and CH₄ lifetimes are functions of the radical OH concentration (reactions 3 and 4). The effect of extremely reduced gas emissions (CO, CH₄, H₂ – dominated), resulting from magmatic intrusions into coaliferous sediments, is therefore to considerably increase both CO and CH₄ lifetimes. In the present lower atmosphere CO, and CH₄ lifetimes are 1.6 months and 5 years, respectively, for a mean OH concentration of 1×10^6 cm⁻³ (Wang et al., 2001). Figure 4a (and Fig.SM3 a, b, c) shows how, after 30 days of gas emissions, CO lifetime increases to 5-20 months at a continental scale and locally close to the emission centre up to 100-1,000 months. CH₄ lifetime increases to 20-100 years at a continental scale and locally close to the emission centre up to 100-10,000 years (Fig.4b, and Fig.SM3 d, e, f). The effect of clouds, which strongly decreases OH concentration, can be observed in Figure 4 at longitudes of 120-160E. The occurrence of clouds reduces photochemical activity (reactions 1 and 2) and therefore increases CO and CH₄ lifetimes.

When a lava flow is associated with magma intrusion, CO and CH₄ lifetimes also depend on NO produced by atmospheric nitrogen oxidation at the lava surface. NO increases ground level ozone production, therefore increasing OH generation (reactions 1 and 2) and decreasing CH₄ and CO lifetimes.

3.4 CH₄ contents in the whole atmosphere

The complementary calculations performed on 100-year duration allow to evaluate the mid-term impact of trap emplacement in terms of methane emissions. Magma production rate (100 km³/yr) and consequent gas emissions (in Table 1) were assumed constant during time and the

lifetime of CH₄ constant in the atmosphere. Figure 5 shows the evolution of the mean CH₄ volume mixing ratio over the whole atmosphere, during and after 10 years of magmatic activity. Calculations using the current mean CH₄ lifetime in the whole atmosphere of 8 years (Fischer et al., 2008) show that a 10 year-lasting magmatic activity would increase CH₄ volume mixing ratio up to 7-19 ppmv (for minimum and maximum gas emissions in Tab.1), 14 to 38 times higher than initial CH₄ concentration, and 3 to 10 times higher than the present one (1.77 ppmv; IPCC, 2007). The amount of time necessary to return initial conditions would be ~50-60 years.

We have seen in section 3.3 that large CO and CH₄ emissions substantially increase CH₄ lifetime, by reducing OH concentration in the atmosphere. For the lower atmosphere, we calculate CH₄ lifetimes between 20 and 100 years at the continental scale (Fig.4 b). Only a global model would realistically estimate the mean increase in CH₄ lifetime in the whole atmosphere as a consequence of 10 years of magmatic activity. Figure 5 gives however an estimation of the effect of increasing CH₄ lifetime on the mean CH₄ volume mixing ratios of the atmosphere and on the time necessary to restore initial conditions (blue, orange and green curves in Fig.5). In the case of maximum gas emissions, CH₄ lifetime increasing to 10, 15 and 20 years would yield mean CH₄ volume mixing ratios in the whole atmosphere of 21, 24 and 26 ppmv, respectively. These values are 42 to 52 times higher than initial methane concentration, and 12 to 15 times higher than the current one (IPCC, 2007). Moreover, the time required to bring back the atmospheric CH₄ volume mixing ratio to the initial value would increase to 75-100 years (Fig.5).

4. Impact on the environment and life

Although volatile emissions during the emplacement of Siberian volcanism/magmatism are still not univocally identified as the cause of the end-Permian crisis (e.g. Knoll et al., 2007;

Brand et al., 2012), several hypotheses exist regarding the related kill mechanisms that impacted both marine and terrestrial environments in apparently distinct ways. Poisoning due to trace metals was suggested by Vogt (1972). Rapid and severe climatic changes and major modifications in marine and terrestrial biota were proposed to result from rapid global cooling caused by the injection of volcanic ash and sulphate aerosols into the atmosphere (e.g. Axelrod, 1981; Roscher et al., 2011). Elevated global atmospheric CO₂ levels were proposed to have led during the end-Permian crisis to climatic conditions inhospitable to both marine and terrestrial life and to hypercapnia (Kiehl and Shields, 2005; Knoll et al., 2007; Retallack and Jahren, 2008; Retallack, 2012; Brand et al., 2012). Strong constraints for these high CO₂ levels come from the stomatal index of fossil leaves (Retallack, 2001, 2012), and the physiological adaptations experienced by marine organisms (Knoll et al., 2007 and references therein). Global warming due to the emission of thermogenic and/or magmatic greenhouse gases was also repeatedly evoked to have affected marine and terrestrial biota (Retallack, 1999, 2001, 2012; Wignall, 2001; Courtillot and Renne, 2003; Kiehl and Shields, 2005; Knoll et al., 2007; Retallack and Jahren, 2008; Brand et al., 2012). Thermogenic emissions of greenhouse gases and halocarbons from the Siberian Traps were also suggested to have caused ozone depletion: the collapse of the ozone layer would have led to high levels of surface radiation causing various biological damages to terrestrial organisms (Svensen et al., 2009). As shown by Knoll et al. (2007), the killer mechanism was probably not unique, but rather a synergy of different perturbations interacting to increase the vulnerability of organisms to environmental changes.

Some assumptions have been necessary to estimate gas fluxes produced during magma-sediment interactions and several simplifications have been used to carry out the atmospheric modelling of these gas emissions in conditions relevant to the emplacement of the Siberian intrusions. Nevertheless, our results clearly point out that after only one month of magmatic

intrusion in coaliferous sediments (i) exceptional concentrations of CO and CH₄ in the lower atmosphere are locally reached, (ii) the lifetimes of these two species in the atmosphere are strongly enhanced relative to pre-magmatic conditions. The effect of 10 years lasting magmatic activity is to increase by a factor of 14 to 38 methane concentration in the whole atmosphere. This effect is even more pronounced if the increase in methane lifetime is taken into account. Hereafter we discuss the most likely environmental implications of these phenomena.

4.1 Local and short term implications

The extremely high volume mixing ratios of carbon monoxide produced by one month of magmatic activity are likely to have had a poisoning effect on end-Permian fauna at a local scale and in the very short term. Unfortunately, we cannot directly estimate the importance of this effect using the present knowledge because all current studies have been conducted on mammals (Penney, 1990; WHO, 2004). Without this crucial information all discussions about the lethal effect of CO are too speculative and the atmospheric modelling of CO dispersion over longer durations than 30 days is worthless. Moreover, detailed studies of Siberian fauna through the end-Permian extinction are currently missing to compare with surveys in other continents (e.g. Ward et al., 2005) to gain information about the “local” effect of CO emissions.

We however stress that the effect of CO on animal health has been observed to strongly depend on the concentration, but also on the time of exposure (WHO, 2004). In our case, exposure times to high concentrations are particularly large, as diurnal variations are very limited due to the lifetime of CO considerably larger than 1 month.

4.2 Global and long term effects

The important increase in both methane lifetime (Fig.4b), and methane concentration in the whole atmosphere (Fig.5) due to magmatic (\pm volcanic) activity at the Siberian Traps has an obvious implication in the enhancement of the global warming potential of the end Permian-early Triassic. Though a precise quantification of this effect for the end-Permian atmosphere is beyond the scopes of this paper, we can nevertheless estimate the radiative forcing (ΔF) in W/m^2 for methane, which expresses the change in the net irradiance of the atmosphere due to the increase in methane concentration. To this aim, we use the empirical equation of Hansen et al. (1988):

$$\Delta F = 0.036 (\sqrt{M} - \sqrt{M_0}) - [f(M, N_0) - f(M_0, N_0)] \quad (10)$$

where M is CH_4 volume mixing ratio in ppbv, M_0 and N_0 are initial volume mixing ratios of CH_4 and N_2O in ppbv (500 and 250 ppbv, respectively as explained in section 2.2.1). $f(M, N)$ are the methane-nitrous oxide overlap terms that account for the significant overlap between some of the infrared absorption bands of these two species:

$$f(M, N) = 0.47 \ln [1 + 2.01 \times 10^{-5} (MN)^{0.75} + 5.31 \times 10^{-15} M (MN)^{1.52}] \quad (11)$$

The equation was obtained for $M < 5000$ ppbv. The volume mixing ratios of CH_4 that we calculate for 10 years of magmatic-volcanic activity vary from 7000 to 26000 ppbv, depending on methane lifetime and on whether minimum or maximum methane production fluxes are considered. Though these values are only speculative because the duration of a single magmatic/volcanic event of the Siberian Traps is not precisely known, we can nevertheless extrapolate equation (10) to estimate the radiative forcing resulting from magmatic activity lasting 10 years, which represent a minimum duration for a single event of large igneous provinces (Chenet et al., 2008). For $M=7000$ and 26000 ppbv, we obtain a radiative forcing of 1.9 and 4.2 W/m^2 , respectively. The lower value (1.9 W/m^2) is comparable to the radiative forcing due to the increase of both CO_2 and CH_4 concentration between 1765 and 1990 (IPCC, 1990), the total radiative forcing of long-life greenhouse gases

for year 2005 being 2.63 W/m^2 (IPCC, 2007). Although very approximated, these calculated values of radiative forcing therefore suggest that methane emissions from magma-organic matter interaction at the Siberian Traps had a high climate perturbation potential. We recall that CO_2 emissions due the interaction of the magma with carbonate rocks during magma rising (and less likely SO_2 and halocarbon emissions due to magma-evaporite interactions) are expected to have accompanied CO and CH_4 emissions (Svensen et al., 2009), and to have therefore increased the total radiative forcing due to greenhouse gases.

The estimation of the Global Warming Potential of methane is particularly complex for the studied context (methane enhances its own lifetime through changes in OH concentration and carbon monoxide also contributes to reduce OH concentration), and will not be attempted.

Methane emissions at the Siberian Traps have been also considered responsible for the marked negative carbon isotope shift observed in both marine and terrestrial sediments at the end of the Permian (Retallack and Jahren, 2008). Recently the occurrence of terrestrial carbon, in the form of char, in marine sediments from the Canadian High Arctic has been considered as a direct testimony of coal combustion at the Siberian Traps (Grasby et al., 2011). This char therefore provides a temporal link between magma-coal interactions at the Siberian Traps and the end-Permian extinction event. Three coal fly ash loading events have been recognized in the Permian sediments deposited immediately before the mass extinction, the first event being synchronous with the beginning of a significant negative $\delta^{13}\text{C}_{\text{org}}$ shift (Grasby et al., 2011), consistent with inorganic and organic records observed globally in both marine and terrestrial sediments (e.g. Payne and Kump, 2007; Retallack and Jahren, 2008; Grasby and Beauchamp, 2008).

As far as we know, the C isotopic signature of CO produced by high temperature interaction between magma and organic matter is currently unconstrained. However, isotopic analyses of graphite from native iron-bearing intrusions indicate very limited fractionation of C between

organic matter and graphite (Ryabov and Lapkovsky, 2010), suggesting a C isotopic signature of CO also similar to that of the organic matter [$\delta^{13}\text{C}_{\text{PDB}}$ from -22.6 to -30‰; Ryabov and Lapkovsky, 2010]. On this basis, we suggest that large amounts of organic matter-derived CO are therefore likely to have contributed to the negative carbon isotopic excursion of the end-Permian. Berner (2002) calculated that 4200 Gt of C released into the atmosphere as methane with a carbon isotopic composition $\delta^{13}\text{C} = -65\text{‰}$ could have accounted for the maximum measured isotopic shift of $\sim 8\text{‰}$ in $\delta^{13}\text{C}$ of the oceans at the Permian-Triassic boundary. If released carbon had a heavier isotopic composition, similar to that of the organic matter, the amount of carbon required to explain the isotopic shift would have been more than double (by classical isotopic mass balance). Considering a $\delta^{13}\text{C}$ comprised between -23 and -30‰ for both CO and CH₄ (Svensen et al., 2009 estimated $\delta^{13}\text{C}$ between -25 and -30‰ for thermogenic methane), we calculate that 800-3000 years of emissions of carbon monoxide and methane with the fluxes indicated in Table 1 would supply the necessary amount of carbon.

Conclusions

LIP eruptions coincide with major mass extinctions (Vogt, 1972; Courtillot and Renne, 2003). The possible causal link has been ascribed to both short and long term effects of volcanic gas emissions (Wignall, 2001; Scaillet, 2008). Here we show that the environmental consequences of magmatic activity are, inter alia, strongly dependent on magma-host rock interactions, in particular when the host rocks are composed of carbonates, sulphates, salts, or organic compounds (as already proposed by Svensen et al., 2004; 2007; 2009; Ganino and Arndt, 2009). Such a mechanism leads to atmospheric injection of volatiles in amounts greatly exceeding the original magmatic content and possibly departing significantly from the redox state of the magma source. The atmospheric modelling of CO-CH₄ dominated gas emissions

resulting from magma-organic matter interactions at the Siberian Traps shows that (i) carbon monoxide levels attained in the low atmosphere at the continental scale were comparable to those currently measured in polluted urban areas (2-5 ppmv), and significantly higher close to the degassing zone (>50 ppmv); (ii) important perturbations of atmosphere chemistry were attained leading to substantial decrease in the radical OH concentration; (iii) CO and CH₄ lifetimes were consequently enhanced (3 to 20 times at the continental scale), therefore increasing the residence time of these two species in the atmosphere. Ten years of magmatic/volcanic activity are calculated to increase by a factor of 10 to 50 the mean concentration of methane in the whole atmosphere, yielding a radiative forcing comparable or superior to that due to the increase of both CO₂ and CH₄ concentration between 1765 and 1990. Short-term poisoning of local fauna by carbon monoxide and long-term global warming by methane are therefore the most likely implications of gas emissions due to magma-organic matter interactions at the Siberian Traps.

References

- Akulov, N.I., 2006. Nodules in carbonaceous sediments of the Southern Tunguska Basin. *Lithology Min. Res.* 41, 73-84.
- Axelrod, D.I., 1981. Role of volcanism in climate and evolution. *Geol. Soc. Am. Spec. Paper* 185, 1-59.
- Berner, R.A., 2002. Examination of hypotheses for the Permo-Triassic boundary extinction by carbon cycle modeling. *Proc. Nat. Acad. Sci.* 99, 4172-4177.
- Brand, U., Posenato, R., Came, R., Affek, H., Angiolini, L., Azmy, K., Farabegoli, E., 2012. The end-Permian mass extinction: a rapid volcanic CO₂ and CH₄-climatic catastrophe. *Chem. Geol.* 322-323, 121-144.
- Chenet, A.L., Fluteau, F., Courtillot, V., 2005. Modelling massive sulphate aerosol pollution, following the large 1783 Laki basaltic eruption. *Earth Planet. Sci. Lett.* 236, 721-731.
- Chenet, A.L., Fluteau, F., Courtillot, V., Gérard, M., Subbarao, K. V., 2008. Determination of rapid Deccan eruptions across the Cretaceous- Tertiary boundary using paleomagnetic

- secular variation: Results from a 1200-m-thick section in the Mahabaleshwar escarpment. *J. Geophys Res.* 113 doi:10.1029/2006JB004635.
- Chumakov, N.M., Zharkov, M.A., 2003. Climate during the Permian–Triassic biosphere reorganizations. Article 2. Climate of the Late Permian and Early Triassic: General inferences. *Strat. Geol. Correl.* 11, 361–375.
- Cockell, C.S., 1999. Crises and extinction in the fossil record—a role for ultraviolet radiation. *Paleobiology* 25, 212–225.
- Coffin, M.F., Eldholm, O., 1994. Large igneous provinces: crustal structure, dimensions, and external consequences. *Rev. Geophys.* 32, 1 – 36.
- Courtillot, V., Renne, P., 2003. On the ages of flood basalt events. *C. R. Geosci.* 335, 113–140.
- Czamanske G.K., Zen'ko T.E., Fedorenko V.A., Calk L.C., Budahn J.R., King B.S.W., Siems D.F., 1995. Petrographic and geochemical characterization of ore-bearing intrusions of the Noril'sk type, Siberia, with discussion of their origin : Tokyo, *Resource Geol. Spec. Iss.*18, Soc. Resource Geol., 1-48.
- Czamanske, G. K., Gurevitch, A. B., Fedorenko, V., Simonov, O., 1998. Demise of the Siberian Plume: Paleogeographic and Paleotectonic Reconstruction from the Prevolcanic and Volcanic Record, North-Central Siberia. *Int. Geol. Rev.* 40, 95-115.
- EDGAR (Emission Database for Global Atmospheric Research) database (<http://edgar.jrc.ec.europa.eu>)
- Ernst, R.E., Buchan, K.L., Campbell, I.H., 2005. Frontiers in Large Igneous Province research. *Lithos* 79, 271-297.
- Erwin, D.H., Bowring, S.A., Yugan, J., 2002. End-Permian mass extinction: a review. In: Koeberl, C., MacLeod, K.G. (Eds.), *Catastrophic events and mass extinctions: Impacts and beyond*. Geological Society of America. Special Paper 356, Boulder, Colorado.
- Erwin, D.H., 2006. *Extinction: How Life on Earth Nearly Ended 250 Million Years Ago*, Princeton University Press, Princeton.
- Fischer, H., Behrens, M., Bock, M., Richter, U., Schmitt, J., Loulergue, L., Chappellaz, J., Spahni, R., Blunier, T., Leuenberger, M., Stocker, T.F., 2008. Changing boreal methane sources and constant biomass burning during the last termination. *Nature* 452, 864-867.
- Freitas, S.R., Longo, K.M., Dias, M.A.F.S., Chatfield, R., Dias, P.S., Artaxo, P., Andreae, M.O., Grell, G., Rodrigues, L.F., Fazenda, A., Panetta, J., 2009. The Coupled Aerosol and Tracer Transport model to the Brazilian developments on the Regional

- Atmospheric Modeling System (CATT-BRAMS) - Part 1: Model description and evaluation. *Atmos. Chem. Phys.* 9, 2843-2861.
- Ganino, C., Arndt, N.T., Zhou, M.-F., Gaillard, F., Chauvel, C., 2008. Interaction of magma with sedimentary wall rock and magnetite ore genesis in the Panzhihua mafic intrusion, SW China. *Mineralium Deposita* 43, 677–694.
- Ganino, C., Arndt, N. T., 2009. Climate changes caused by degassing of sediments during the emplacement of large igneous province. *Geology* 37, 323-326.
- GEIA (Global Emissions Inventory Activity) database (<http://www.geiacenter.org/>)
- Grasby, S. E., Beauchamp, B., 2008. Intrabasin variability of the carbon-isotope record across the Permian-Triassic transition, Sverdrup Basin, Arctic Canada. *Chem. Geol.* 253, 141-150.
- Grasby, S.E., Sanei, H., Beauchamp, B., 2011. Catastrophic dispersion of coal fly ash into oceans during the latest Permian extinction. *Nature Geosci.* DOI : 10.1038/NGEO01069.
- Grell, G. A., 1993. Prognostic evaluation of assumptions used by cumulus parameterizations, *Mon. Wea. Rev.*, 121, 764-787.
- Grell, G. A., Dévényi, D., 2002. A generalized approach to parameterizing convection combining ensemble and data assimilation, *Geophys. Res. Lett.*, 29, 1693, doi:10.1029/2002GL015311.
- Hansen, J., Fung, I., Lacis, A., Rind, D., Lebedeff, S., Ruedy, R., Russell, G., 1988. Global climate changes as forecast by Goddard Institute for Space Studies Three Dimensional Model. *J. Geophys. Res.* 93, 9341-9364.
- Huebert, B., Vitousek, P., Sutton, J., Elias, T., Heath, J., Coeppicus, S., Howell, S., Blomquist, B., 1999. et al. Volcano fixes nitrogen into plant available forms. *Biogeochem.* 47, 111-118.
- Iacono-Marziano, G., Gaillard, F., Pichavant, M., 2007. Limestone assimilation and the origin of CO₂ emissions from the Alban Hills (Central Italy): constraints from experimental petrology. *J. Volcanol. Geotherm. Res.* 166, 91-105.
- Iacono-Marziano, G., Gaillard, F., Scaillet, B., Pichavant, M., Chiodini, G., 2009. Role of non-mantle CO₂ in the dynamics of volcano degassing: The Mount Vesuvius example. *Geology* 37, 319-322.

- Iacono-Marziano, G., Gaillard, F., Scaillet, B., Polozov, A.G., Marecal, V., Pirre, M., Arndt, N., submitted to EPSL. Extremely reducing conditions reached during basaltic intrusion in organic matter-bearing sediments.
- Intergovernmental Panel on Climate Change (IPCC), 1990. *Climate Change: The IPCC Scientific Assessment*, edited by J.T. Houghton, G.J. Jenkins, and J.J. Ephraums, 1990, Cambridge University Press, Cambridge, 365 p.
- Intergovernmental Panel on Climate Change (IPCC), 2007. *Contribution of Working Group I to the Fourth Assessment Report of the Intergovernmental Panel on Climate Change*. Edited by Solomon, S., Qin, D., Manning, M., Chen, Z., Marquis, M., Averyt, K.B., Tignor, M., Miller, H.L., Cambridge University Press, Cambridge, 996 p.
- Jambon A., 1994. Earth degassing and large-scale geochemical cycling of volatile elements. *Rev. Mineral.* 30, 479-517.
- Kaminski, E., Chenet, A.-L., Jaupart, C., Courtillot, V., 2010. Rise of volcanic plumes to the stratosphere aided by penetrative convection above large lava flows. *Earth Planet. Sci. Lett.* 301, 171-178.
- Kiehl, J.T., Shields, C.A., 2005. Climate simulation of the latest Permian: Implications for mass extinction. *Geology* 33, 757-760.
- Knoll, A.H., Bambach, R.K., Payne, J.L., Pruss, S., Fischer, W.W., 2007. Paleophysiology and end-Permian mass extinction. *Earth Planet. Sci. Lett.* 256, 295-313.
- Korte, C., Pande, P., Kalia, P., Kozur, H.W., Joachimski, M.M., Oberhänsli, H., 2010. Massive volcanism at the Permian-Triassic boundary and its impact on the isotopic composition of the ocean and atmosphere. *J. Asian Earth Sci.* 37, 293-311.
- Kuznetsov, V.G., 1997. Riphean hydrocarbon reservoirs of the Yurubchen–Tokhom Zone, Lena-Tunguska Province, NE Russia. *J. Petrol. Geol.* 20, 459–474.
- Mather, T.A., Allen, A.G., Davison, B.M., Pyle, D.M., Oppenheimer, C., McGonigle, A.J.S., 2004. Nitric acid from volcanoes. *Earth Planet. Sci. Lett.* 218, 17-30.
- Matukhin, R.G., 1991. Devonian and Lower Carboniferous [sediments] of the Siberian craton (composition, sedimentation conditions and ore potential). Novosibirsk. Nauka Publisher, Siberian Branch. 164 p. (in Russian)
- Mellor, G., Yamada, T., 1982. Development of a turbulence closure model for geophysical fluid problems, *Rev. Geophys.*, 20, 851–875.

- Mitchell, C., Fitton, J.G., Al'Mukhamedov, A.I., Medvedev, A.I., 1994. The age and duration of flood basalt magmatism: geochemical and palaeomagnetic constraints from the Siberian Province. *Min. Mag.* 58A, 617–618.
- Payne, J.L., Kump, L.R., 2007. Evidence for recurrent Early Triassic massive volcanism from quantitative interpretation of carbon isotope fluctuations. *Earth. Planet. Sci. Lett.* 256, 264–277.
- Penney, D.G., 1990. Acute carbon monoxide poisoning: animal models: A review. *Toxicology* 62, 123-160.
- Petrychenko, O.Y., Peryt, T.M., Chechel, E.I., 2005. Early Cambrian seawater chemistry from fluid inclusions in halite from Siberian evaporites. *Chem. Geol.* 219, 149-161.
- Rees, P.M., Ziegler, A.M., Gibbs, M.T., Kutzbach, J.E., Behling, P.J., Rowley, D.B., 2002. Permian phytogeographic patterns and climate data/model comparison. *J. Geol.* 110, 1-31.
- Reichow et al., 2002 Reichow, M. K., Saunders, A. D., White, R. V., Pringle, M. S., Al'Mukhamedov, A. I., Medvedev, A., Korda, N., 2002. New ^{40}Ar - ^{39}Ar data on basalts from the West Siberian Basin: Extent of the Siberian flood basalt province doubled. *Science* 296, 1846-1849.
- Retallack, G.J., 1999. Post-apocalyptic greenhouse paleoclimate revealed by earliest Triassic paleosols in the Sydney Basin, Australia. *Geol. Soc. Am. Bull.* 111, 52–70.
- Retallack, G.J., 2001. A 300-million-year record of atmospheric carbon dioxide from fossil plant cuticles. *Nature* 411, 287-290.
- Retallack, G.J., 2012. Permian and Triassic greenhouse crises. *Gondwana Research*, in press.
- Retallack, G.J., Krull, E.S., 2006. Carbon isotopic evidence for terminal-Permian methane outbursts and their role in extinctions of animals, plants, coral reefs, and peat swamps. In: Greb, S.F., DiMichele, W.A. (Eds.), *Wetlands through time*. Geological Society of America. Special Paper 399
- Retallack, G., Jahren, A.H., 2008. Methane release from igneous intrusion of coal during Late Permian extinction events. *J. Geol.* 116, 1–20.
- Roscher M., Stordal, F., Svensen, H., 2011. The effect of global warming and global cooling on the distribution of the latest Permian climate zones. *Palaeogeography, Palaeoclimatology, Palaeoecology*, 309, 186-200.
- Ryabov, V. V., Lapkovsky A. A., 2010. Native iron (-platinum) ores from the Siberian Platform trap intrusions. *Austral. J. Earth Sci.* 57, 707-736.

- Saal, A.E., Hauri, E.H., Langmuir, C.H., Perfit, M.R., 2001. Vapour undersaturation in primitive mid-ocean-ridge basalt and the volatile content of Earth's upper mantle. *Nature* 419, 451-455.
- Scaillet, B., Macdonald, R., 2006. Experimental and thermodynamic constraints on the sulphur yield of peralkaline and metaluminous silicic flood eruptions. *J. Petrol.* 47, 1413-1437.
- Scaillet, B., 2008. Geochemistry – Are volcanic gases serial killers? *Science* 319, 1628-1629.
- Sobolev, S.V., Sobolev, A.V., Kuzmin, D.V., Krivolutsкая, N.A., Petrunin, A.G., Arndt, N.T., Radko, V.A., Vasiliev, Y.R., 2011. Linking mantle plumes, large igneous provinces and environmental catastrophes. *Nature* 477, 312-316.
- Svensen, H., Planke, S., Malthes-Sørensen, A., Jamtveit, B., Myklebust, R., Eidem, T., Rey, S.S., 2004. Release of methane from a volcanic basin as a mechanism for initial Eocene global warming. *Nature* 429, 542–545.
- Svensen H., Planke, S., Chevallerier, L., Malthes-Sørensen, A., Corfu, B., and Jamtveit, B., 2007. Hydrothermal venting of greenhouse gases triggering Early Jurassic global warming. *Earth Planet. Sci. Lett.* 256, 554–566.
- Svensen, H., Planke S., Polozov A.G., Schmidbauer N., Corfu F., Podladchikov Y.Y., Jamtveit B. 2009. Siberian gas venting and the end-Permian environmental crisis. *Earth Planet. Sci. Lett.* 277, 490–500.
- Thordarson, T., Self, S., 2003. Atmospheric and environmental effects of the 1783– 1784 Laki eruption: A review and reassessment. *J. Geophys. Res.* 108, doi:10.1029/2001JD002042.
- Toon, O.B., McKay, C.P., Ackerman, T.P., Santhanam, K.L., 1989. Rapid calculation of radiative heating rates and photodissociation rates in inhomogeneous multiple scattering atmospheres. *J. Geophys. Res.*, 94, 16287-16301.
- Visscher, H., Looy, C.V., Collinson, M.E., Brinkhuis, H., Cittert, J., Kurschner, W.M., Sephton, M.A., 2004. Environmental mutagenesis during the end-Permian ecological crisis. *Proc. Natl. Acad. Sci. U. S. A.* 101, 12952–12956.
- Vogt, P.R., 1972. Evidence for global synchronism in mantle plume convection, and possible significance for geology. *Nature* 240, 338-342.
- Wallace, P.J., 2005. Volatiles in subduction zone magmas; concentration and fluxes based on melt inclusion and volcanic gas data. *J. Volcanol. Geotherm. Res.* 140, 217-240.

- Walko, R. L., Cotton, W. R., Meyers, M. P., Harrington, J.Y., 1995. New RAMS cloud microphysics parameterization, Part I: the single-moment scheme, *Atmos. Res.*, 38, 29–62.
- Walko, R.L., Tremback, C.J., 2005: ATMET Technical Note 1, Modifications for the Transition from LEAF-2 to LEAF-3, ATMET, LLC, Boulder, Colorado 80308-2195, <http://www.atmet.com/html/docs/rams/2005>.
- Wang, K.Y., Pyle, J.A., Shallcross, D.E., and Larry, D.J., 2001. Formulation and evaluation of IMS, an interactive three-dimensional tropospheric chemical transport model, 2. model chemistry and comparison of modeled CH₄, CO and O₃ with surface measurements. *J. Atmos. Chem.* 38, 31-71.
- Ward, P.D., Botha, J., Buick, R., De Kock, M.O., Erwin, D.E., Garrison, G.H., Kirschvink, J.L., Smith, R., 2005. Abrupt and gradual extinction among late Permian land vertebrates in the Karoo Basin, South Africa. *Science* 307, 709-714.
- Wignall, P. B., 2001 Large igneous provinces and mass extinctions. *Earth Sci. Rev.* 53, 1-33.
- WHO, World Health Organisation, Carbon monoxide (2nd Edition). *Environmental Health Criteria* 213, pp 464. ISBN 9241572132 (2004).

Acknowledgements

G.I.M. was funded by the European Community's Seventh Framework Programme (grant agreement n° PIEF-GA-2008-220926). F.G. is supported by the ERC contract n°279790. The numerical simulations were performed on the cluster of the Centre de Calcul Scientifique en Région Centre. CATT-BRAMS is free software provided by CPTEC/INPE and distributed under the CC-GNU-GPL license. We thank Roberto Salzano for his useful advice. We thank B. Marty for the careful handling of the manuscript, H. Svensen and an anonymous reviewer for their constructive comments that greatly improved the paper.

Figure Legends

Fig. 1

Geological map of the Tunguska Basin, Eastern Siberia showing the current distribution of effusive (lava flows and volcanoclastic rocks) and intrusive rocks (modified from Malich et

al., 1974). The Tunguska Basin sediments include petroleum accumulations in the Neoproterozoic to Carboniferous units (Kuznetsov, 1997) and numerous coal seams in the Late Carboniferous-Permian strata (Czamanske et al., 1998). Shaded areas illustrate the approximate extent of Cambrian and Devonian evaporites (Zharkov, 1984; Petrychenko et al., 2005). The locations of the native iron-bearing intrusions are also shown (Ryabov and Lapkovsky, 2010).

Fig.2

Schematic illustration (not to scale) of magma rising in the North and North-west of the Siberian Platform, of the intrusion into the coaliferous sediments and of the possible, although unconfirmed, magma extrusion with formation of a lava flow. Three types of magma-sediment interactions are probable at different stratigraphic levels: (a) magma-carbonate interactions leading to the breakdown of carbonates; (b) magma-petroleum interactions causing destabilization of hydrocarbons in the contact aureoles (Svensen et al., 2009), reduction of the magma redox state and possible graphite crystallization; (c) magma-coal interactions also triggering hydrocarbon destabilization and a strong reduction of the magma redox state, accompanied by graphite and native iron crystallization.

Fig.3

CO (a, b, c) and CH₄ (d, e, f) propagation in North Asia after 30 days that the gases produced by magma intrusion arrive at surface. Volume mixing ratios in the first layers of the atmosphere (0-30m) are expressed in ppmv. Three scenarios have been investigated: (a, d) magmatic intrusion without lava flow, maximum fluxes presented in Table 1; (b, e) magmatic intrusion without lava flow, minimum fluxes presented in Table 1; (c, f) magmatic intrusion accompanied by lava flows and temperature perturbation at surface, minimum fluxes presented in Table 1. The white square indicates an area of $2 \times 10^6 \text{ km}^2$.

Fig.4

CO lifetimes in months (a), and CH₄ lifetimes in years (b) in the first layers of the atmosphere (0-30 m). Both lifetimes are calculated for maximum fluxes presented in Table 1, in the case of magmatic intrusion without lava flow, after 30 days of gas emissions.

Fig.5

Evolution of CH₄ volume mixing ratio with time, in response to 10 years lasting magmatic activity, calculated for minimum and maximum fluxes (Table1) and different CH₄ lifetimes indicated in the legend.

1 **Table 1. Calculated gas emissions due to magma-sediment interactions.**

2

Emitted species	Intrusion min fluxes (g/yr) ^a	Intrusion max fluxes (g/yr) ^a	Intrus.+lava flow min fluxes (g/yr) ^b	Intrus.+lava flow max fluxes (g/yr) ^b	Without assimilation ^c
CO	3×10^{15}	$1 \times 10^{16*}$	4×10^{15}	$1 \times 10^{16*}$	5×10^{13}
CO ₂	2×10^{14}	2×10^{14}	3×10^{12}	4×10^{12}	9×10^{14}
H ₂	1×10^{14}	1×10^{14}	1×10^{14}	2×10^{14}	6×10^{11}
H ₂ O	8×10^{13}	1×10^{14}	2×10^{12}	2×10^{12}	2×10^{14}
H ₂ S	5×10^{13}	7×10^{13}	1×10^{12}	3×10^{12}	7×10^{13}
CH ₄	4×10^{13}	6×10^{13}	1×10^{12}	1×10^{12}	3×10^6
S ₂	8×10^9	2×10^{10}	2×10^8	2×10^9	5×10^{13}
SO ₂	2×10^7	5×10^7	6×10^3	2×10^4	8×10^{13}
NO ^{**}			$1 \times 10^{12**}$	$5 \times 10^{12**}$	
CH ₄ ^{***}	$3 \times 10^{15***}$	$9 \times 10^{15***}$	$3 \times 10^{15***}$	$9 \times 10^{15***}$	
Tot	7×10^{15}	2×10^{16}	7×10^{15}	2×10^{16}	1×10^{15}

3 a) Fluxes resulting at 10 MPa from high temperature assimilation of 0.5 wt% organic matter (ensuring coexistence of graphite and
 4 native iron). Given ranges account for the variations in initial conditions (initial fO₂ and gas fraction of the magma) and type of organic
 5 matter assimilated, i.e. CH or CH₂ (Iacono-Marziano et al., submitted to EPSL).

6 b) Fluxes resulting at 0.1 MPa from high temperature assimilation of 0.6 wt% organic matter (ensuring coexistence of graphite and
 7 native iron). Given ranges account for the variations in initial conditions (initial fO₂ and gas fraction of the magma) and type of organic
 8 matter assimilated, i.e. CH or CH₂ (Iacono-Marziano et al. , submitted to EPSL).

9 c) Fluxes resulting at 10 MPa from the degassing of a basaltic magma (initial H₂O, CO₂ and S contents of 0.50, 0.08 and 0.10 wt%,
 10 respectively) without assimilation.

11 *) CO fluxes include the contribution of volatilization of graphite and native iron formation according to reaction (3) in (Iacono-
 12 Marziano et al. , submitted to EPSL).

13 **) NO fluxes resulting from nitrogen fixation at the lava surface.

14 ***) Fluxes resulting from contact metamorphism of carbonaceous rocks, calculated following Svensen et al. (2009)

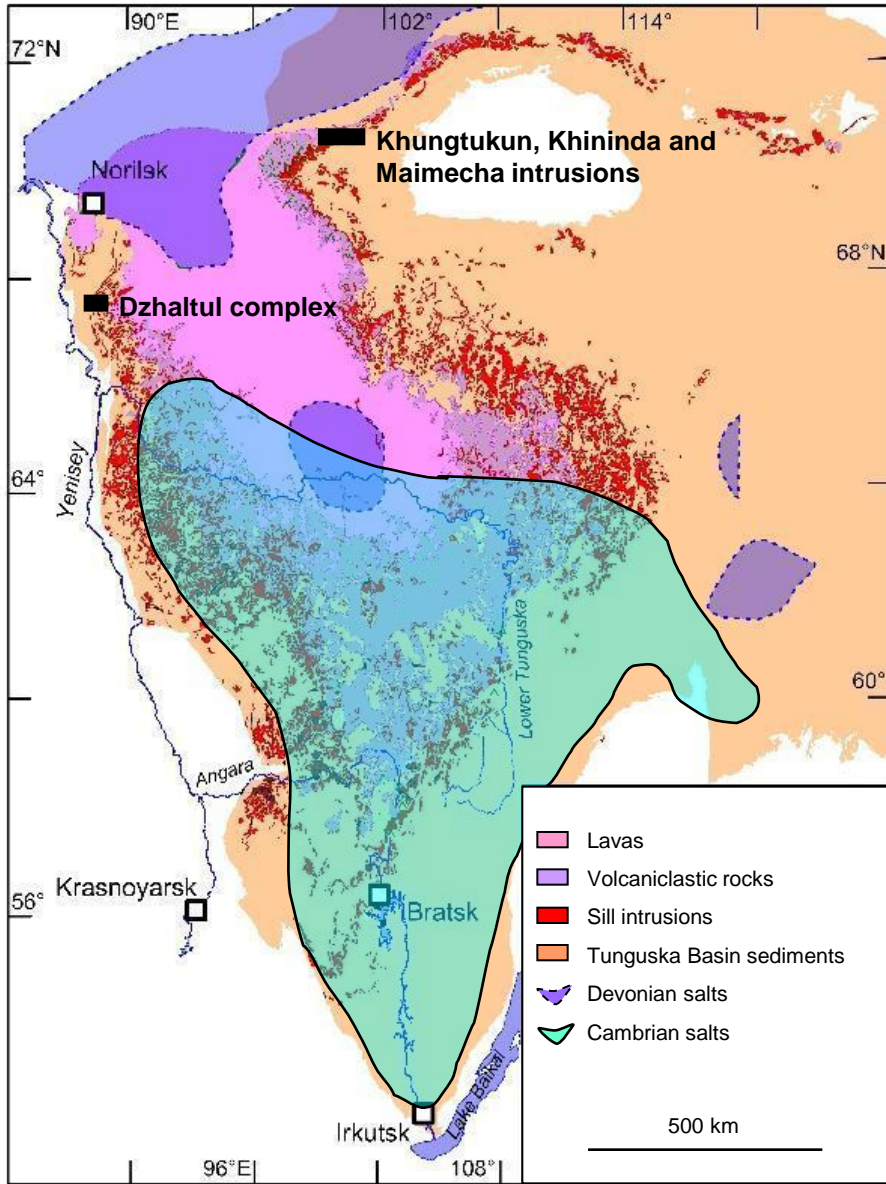
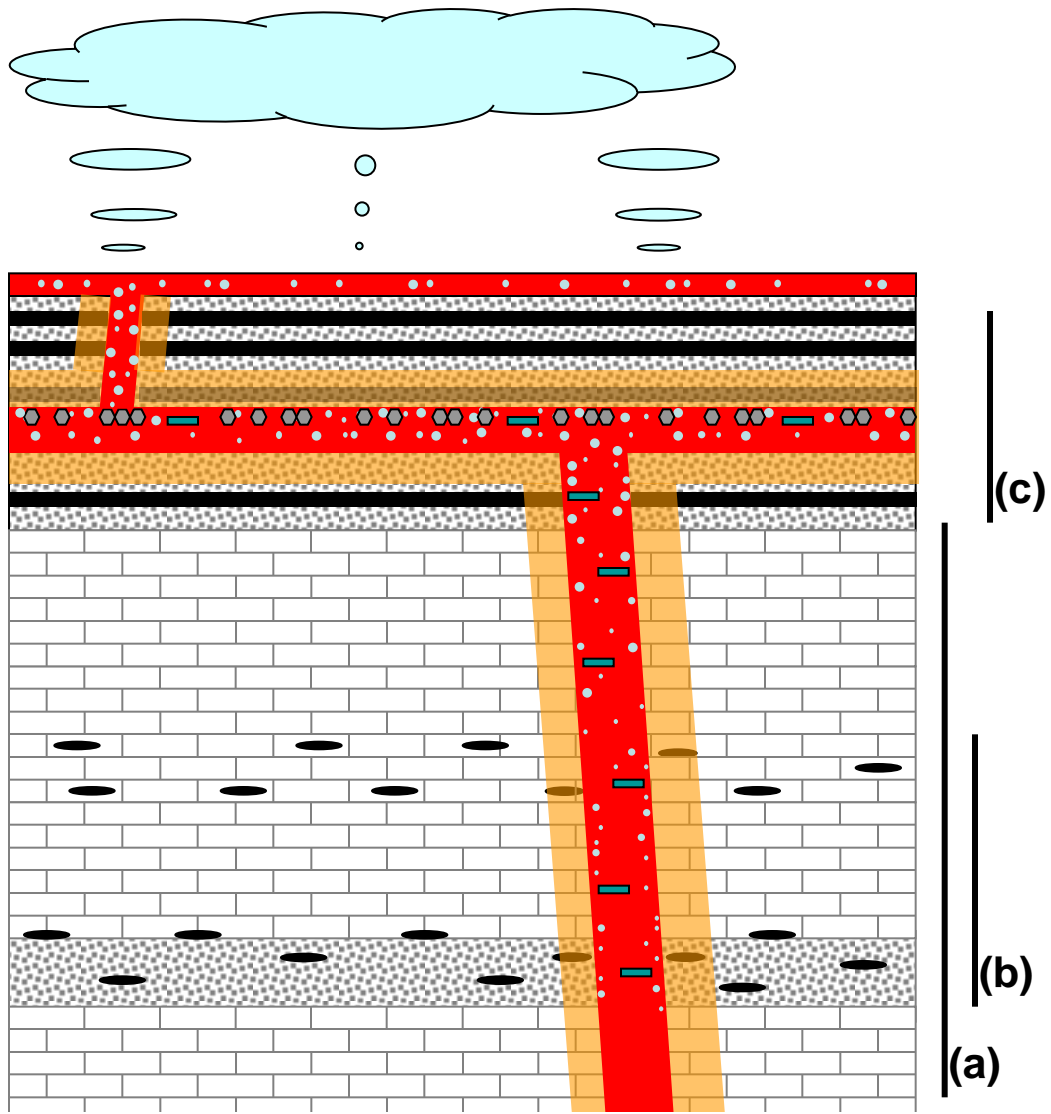


Fig.1





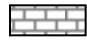



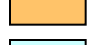


- | | |
|---|---|
|  Sandstones |  Coal |
|  Carbonate rocks and shales |  Petroleum |
|  Magma |  Native iron |
|  Metamorphic aureoles |  Graphite |
|  CO-CH ₄ -dominated gases | |

Fig.2

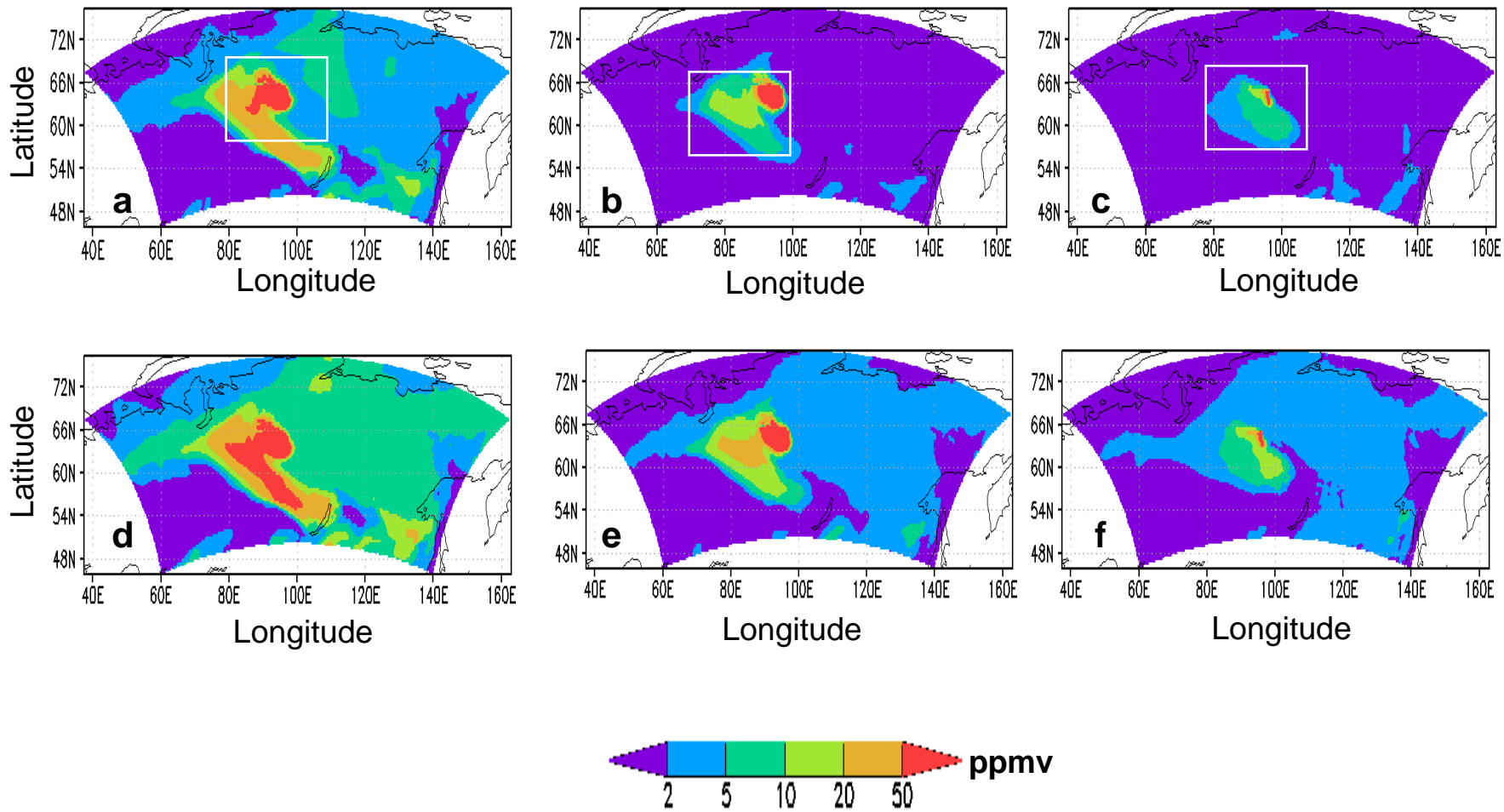


Fig.3

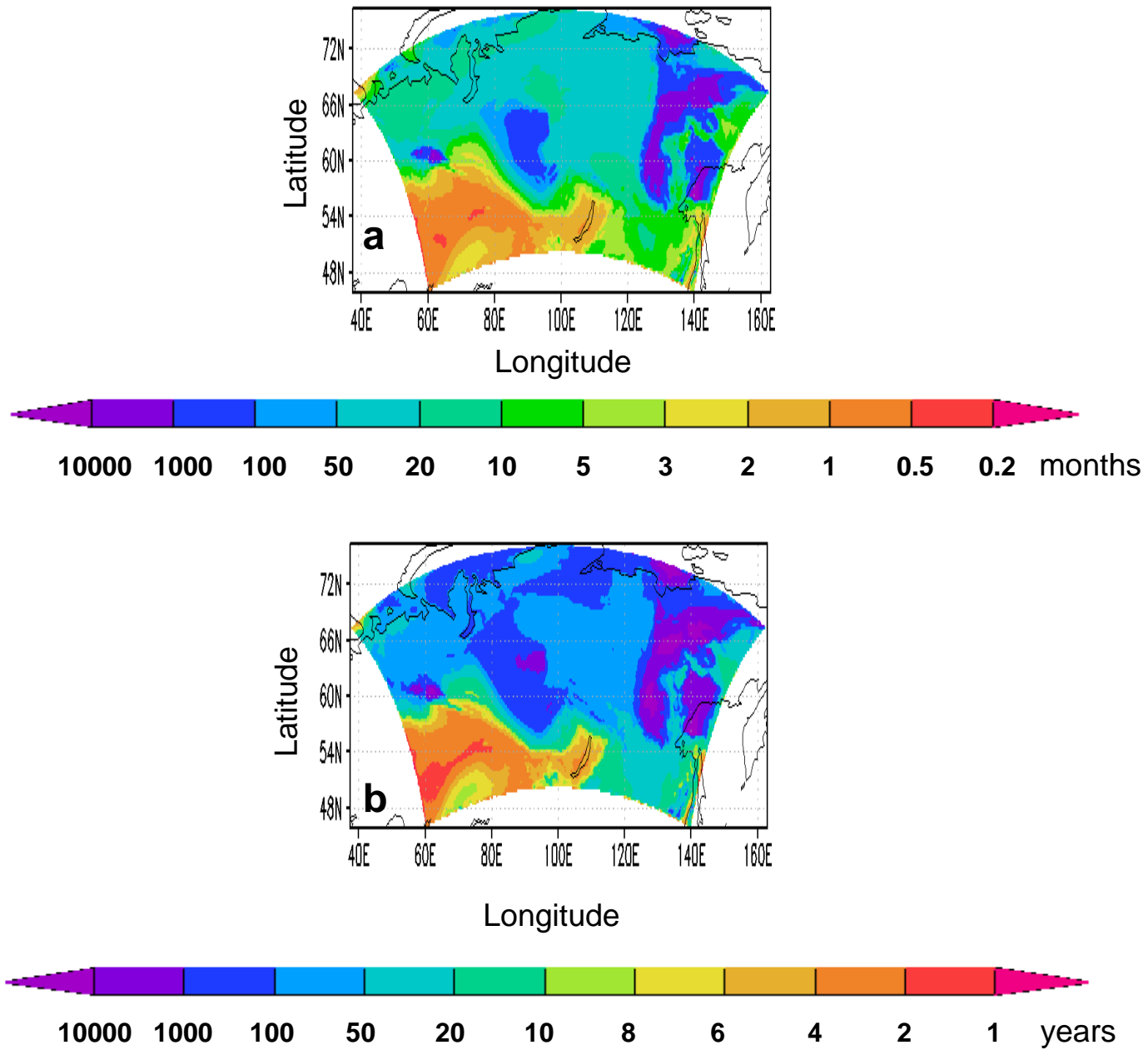


Fig.4

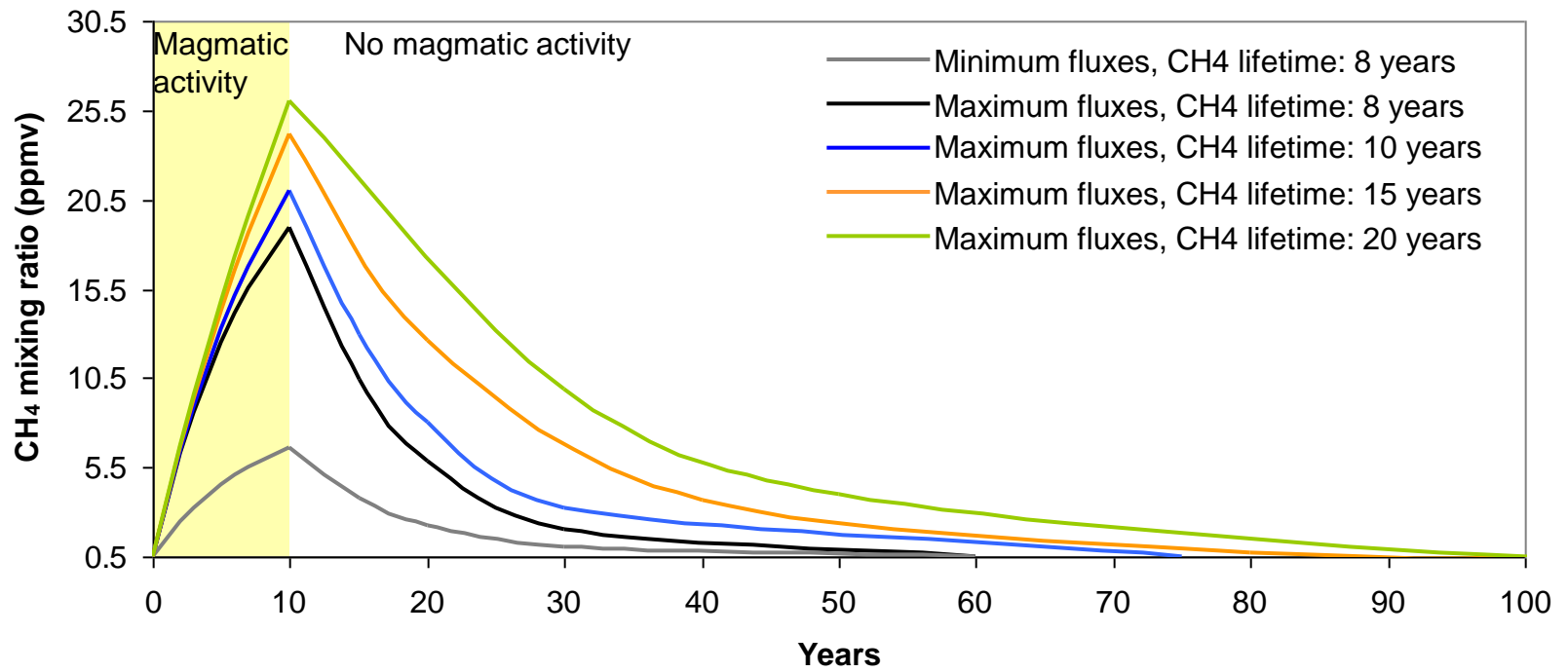


Fig.5